Indian Journal of Radio & Space Physics
Vol. 37, October 2008, pp. 303-311

Limitations of the utility of CMEs for forecasting timings and magnitudes of geomagnetic Dst storms

R P Kane
Instituto Nacional de Pesquisas Espaciais – INPE, C.P. 515, 12245-970 – São José dos Campos, SP, Brazil
kane@dge.inpe.br

Received 11 June 2007; revised 14 May 2008; accepted 14 August 2008

Results of the examination of data for about 100 events in solar cycle 23 (1996 onwards), when CMEs (Coronal Mass Ejections) and IP (Interplanetary) shocks could be matched, are presented. The CMEs had a large range of speed (200-4000 km/s), but the slow CMEs seemed to be accelerated and the fast ones decelerated during the transit from Sun to Earth. Hence, IP shock speed near the Earth was in a narrower range (350-2000 km/s). A regression equation can be established between the CME lateral expansion speed and the corresponding IP shock speed. But observed values have a considerable scatter and can have extreme deviations of ~ 35% from the predicted values. Similarly, the transit times from Sun to Earth can have extreme deviations of ~ 35% from the predicted values. The transit times can be as low as 25 h (extreme uncertainty ~ 5 h) to as high as 100 h (extreme uncertainty ~35 h) and have no one-to-one relationship with the magnitudes of the Dst storms that follow, or with the time intervals between the IP shock and the following maxima of negative Bz or negative Dst. The time intervals between maximum negative Bz and maximum negative Dst are mostly in the range of 0-5 h. The magnitudes of the maxima of negative Bz and the following negative Dst are highly correlated, indicating this as a major, overpowering relationship for determining the severeness of geomagnetic storms.

Keywords: Flares and mass ejections, Coronal mass ejections, Solar-planetary relationships, Geomagnetic storms

PACS No.: 96.60.ph; 96.60.qe

1 Introduction

Geomagnetic storms occur when Earth encounters abnormal interplanetary structures having a substantial negative (southward) Bz component of the interplanetary magnetic field B. This feature was explained by Dungey[1] as follows. When Bz is negative, a neutral point is formed at the dayside magnetopause and the magnetic flux loaded with solar wind plasma is transported to the magnetotail. This plasma is energized by magnetic reconnection at a neutral point formed in the near Earth magnetotail (at about 100 Earth radii) and eventually injected into the magnetosphere. Low energy particles spiral around the stretched geomagnetic field lines and impinge on the terrestrial atmosphere in the Polar Regions, causing enhanced aurora. Higher energy particles rush towards the Earth, but are diverted around the Earth in circular orbits in the equatorial plane and cause large geomagnetic field reductions (Dst, storm-time disturbance depression of several tens of nT).

When CMEs leave the surface of the Sun, they travel outside and the faster ones impinge on the background slow solar wind to form IP (interplanetary) shocks, which move very fast (~ 450-2000 km/s), with plasma densities large (exceeding ~ 10 particles/cc) and with magnetic structures with total field B of several tens of nT. This B is composed of three components, namely, B_x (along the Sun-Earth line), B_Y (perpendicular to B_x but in the Earth´s orbital plane around the Sun) and B_Z, (perpendicular to both B_x and B_Y), the B_z being parallel to Earth´s magnetic axis. When B_Z is large and negative, solar plasma has an entry to the inner magnetosphere as envisaged in the Dungey mechanism described above.

Since severe storms cause damages to electrical installations and communication systems in high latitudes, a warning of the likely occurrence of such storms with some antecedence would be very useful. A possible relation between solar flare acitivity and geomagnetic disturbances was surmised more than a century back (Carrington[2], Hodgson[3]). Hale[4] claimed such a relationship clearly. Chapman and Bartels[5] suggested that on some occasions like the eruptions of solar flares, the Sun probably emits corpuscular

radiation (particles), which may reach the Earth in a few tens of hours (or days). Not all solar flares (even strong ones) were geoeffective, but flares in the western longitudes of the Sun were more effective. Parker[6] proposed the idea of solar wind and envisaged (confirmed later by satellite observations) that the general solar magnetic field of about one gauss would be stretched out in the solar equatorial plane along Archimedes spiral configurations, along which solar material could reach the Earth easily. Further breakthrough came when Tousey[7] identified the Coronal Mass Ejection (CME) phenomenon in the OSO-7 data. A copious data set for CMEs is now available from the Solar and Heliospheric Observatory (SOHO) mission's Large Angle and Spectrometric Coronagraph (LASCO), which images the corona continuously since 1996, covering a field from 1.5 *R*s to 32 *R*s (solar radius).

Gopalswamy *et al.*[8,9] studied the solar cycle variation of various properties of CMEs for a part of cycle 23 (1996–2002) and reported an order of magnitude increase (12 times) in CME rate from solar minimum (1996) to solar maximum (2002). The CMEs are numerous and at solar maximum, these can be seen as many as 5-6 events per day. Since these are emitted at different solar longitudes, very few are encountered by the Earth. However, a subset of these, namely the halo CMEs seem to be spreading all around the solar disc in wide angles and have a good chance of encountering the Earth. The lateral (sideward) expansion of the halo CMEs can be monitored for outgoing speeds, which are generally several thousand kilometers per second.

Using interplanetary data where specific ICMEs (Interplanetary CMEs) could be related to specific CMEs at the Sun, a correlation analysis of 38 events (Dal Lago *et al.*[10]) indicated a relationship $V_{eje} = 335 + 0.21\ V_{exp}$, where V_{eje} is the ICME ejecta speed at 1 AU (Earth´s orbit around the Sun) and V_{exp} is the lateral expansion speed of the halo CMEs. However, though the correlation coefficient was high (+ 0.78), the scatter was large. Manoharan *et al.*[11] and Manoharan[12] studied 91 interplanetary (IP) shocks associated with coronal mass ejections (CMEs) originating within about ± 30 in longitude and latitude from the center of the Sun during 1997-2002. These CMEs covered a wide range of initial speeds of about 120-2400 km/s. However, the plot of the observed IP shock speed at 1 AU against initial speed of the CME showed considerable scatter. Schween *et al.*[13] also report a similar scatter. The extent of this scatter would indicate the limitation of CMEs as a useful tool for forecasting timings of geomagnetic storms. In the present communication, data for about hundred CMEs and associated ICME shocks in solar cycle 23 are examined critically, to set the limits of utility of CMEs for forecasting. Also, once the shock is detected, the time-delay up to the maximum negative Dst that follows, is also examined.

2 Source of data

Data were obtained from the list of IP shocks and associated CMEs given by Manoharan *et al.*[11] and Manoharan[12] (2006) and from http://www.srl.caltech.edu/ACE/ASC/level2/index. html of ACE level 2 (verified) data for interplanetary magnetic field. For Dst, the Japanese WDC (Kyoto) website http://swdcwww.kugi.kyoto-u.ac.jp/aeasy/index.html of Japanese WDC at Kyoto has given 1-min data for ASY/SYM indices, where the symmetrical index SYM is the Dst. The CMEs associated with the shocks were identified using white-light measurements obtained from Large Angle and Spectrometric Coronagraph (LASCO) and full disk images from Extreme Ultraviolet Imaging Telescope (EIT) on board Solar Heliospheric observatory (SOHO) mission. For an IP shock at the Earth, its potential CME near the Sun was identified within a time frame of 1-5 days, backward from the onset time of the shock. (The possibility of some erroneous matching cannot be ruled out).

For each one of about hundred CME-ICME pairs, the parameters examined were as follows:

(i) The CME lateral expansion speed V_{cme} is as given in Manoharan *et al.*[11] and Manoharan[12]. The CME-ICME association has been done fairly rigorously as described in Manoharan *et. al.*[11], but briefly, the IP (Interplanetary) shocks considered were associated with CMEs originating close to the center of the Sun, within about 30° from the Sun's center.

(ii) The transit time from Sun to the Wind or ACE spacecraft locations

(iii) The velocity V_{sh} of the IP shocks.

(iv) The time intervals between the UT time of IP shock arrival and the UT timings of the subsequent maximum negative deviations of the Bz component of interplanetary field (Shock-Bz) and of geomagnetic Dst (Shock-Dst) as also the time interval Bz-Dst.

Table 1—Intercorrelations of the various parameters for 103 events

	V_{sh}	Transit	V_{cme}	Shock-Bz	Bz-Dst-	Shock-Dst	Bz, nT	Dst, nT	V_{sh}.Bz
V_{sh}	1.00								
Transit	– 0.62	1.00							
V_{cme}	0.69	– 0.68	1.00						
Bz-Shock	– 0.22	0.06	– 0.20	1.00					
Dst-Bz	0.28	– 0.08	0.21	– 0.29	1.00				
Dst-Shock	– 0.10	0.03	– 0.11	0.90	0.16	1.00			
Bz	– 0.57	0.51	– 0.55	0.26	– 0.03	0.25	1.00		
Dst	– 0.50	0.50	– 0.47	0.18	– 0.03	0.17	0.85	1.00	
V_{sh}.Bz	– 0.85	0.53	– 0.69	0.24	– 0.20	0.16	0.86	0.73	1.00

(v) The magnitudes of maximum negative values of Bz and Dst

(vi) The product V_{sh}Bz.

3 Correlations

Table 1 gives the inter-correlations of these parameters for 103 events. The following may be noted in Table 1:

(a) The CME lateral expansion speeds (V_{cme}) have a fairly good (but not very high) correlation (+ 0.69) with the shock speed V_{sh} as shown in Fig. 1. The small dots are for individual events and the big dots with standard deviations are for ranges (average of 15 pairs). A curious aspect is that the relationship is not uniformly linear, as was implied in Dal Lago *et al.*[10]. In fact, for Vcme values in the range 200-800 km/s, the V_{sh} values are almost constant on the average near ~ 500 km/s, consistent with the empirical model of Gopalswamy *et al.*[14,15], which states that slow CMEs are accelerated and fast CMEs are decelerated toward the ambient solar wind speed of ~ 400 km/s. However, there is a large scatter in individual values. Further, above the V_{cme} value of ~ 800 km/s, there is an indication of linear relationship, but the scatter is very large. (Incidentally, for all the events, the correlation coefficient of + 0.69 is largely influenced by the single event of 29 Oct. 2003 Halloween event, when V_{cme} was ~ 4000 km/s and V_{sh} was ~ 2000 km/s. If this event is omitted, the correlation drops to + 0.55). For data excluding the 29 Oct. 2003 event, Manoharan *et al.*[11] have fitted a quadratic, as follows

$$V_{sh} = 420 + 0.2\ V_{cme} + 2.3 \times 10^{-5}\ V^2_{cme}$$

However, the scatter around this regression line is very large. Around the big dots in Fig. 1, the standard deviations and ranges are as given in Table 2. Thus, actual values can differ from the regression prediction with a standard deviation of ~ 20% and an extreme deviation of ~ 35%.

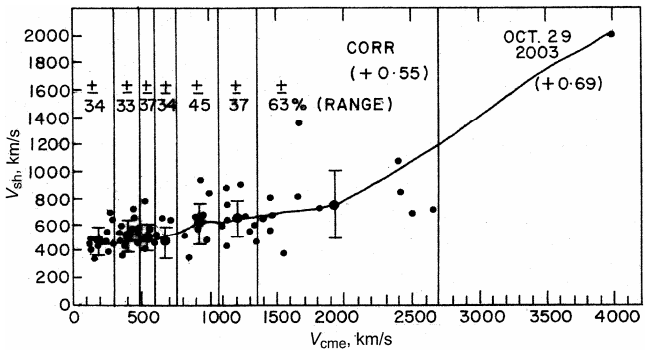

Fig. 1—Plot of IP (Interplanetary) Shock speed V_{sh} *vs* CME (Coronal Mass Ejection) lateral expansion speed V_{cme} [The small dots are for individual events and the big dots with standard deviations are for ranges (average of 15 pairs)]

Table 2—Averages of V_{sh} for ascending values of V_{cme}

V_{cme}, km/s	V_{sh}, km/s		
	Average	Standard deviation	Range
209	485	±87 (18%)	±166 (34%)
399	522	±101 (19%)	±172 (33%)
527	507	±100 (20%)	±190 (37%)
663	494	±96 (19%)	±170 (34%)
926	622	±161 (26%)	±280 (45%)
1186	643	±148.(23%)	±240 (37%)
1864	767	±243 (32%)	±480 (63%)
4000	2000	Single event	Single event

(b) The CME expansion speeds (V_{cme}) have a fairly good (but not very high) negative correlation (– 0.68) with the transit time T_{sh} as shown in Fig. 2. The small dots are for individual events and the big dots with standard deviations are for ranges (average of 15 pairs). Manoharan *et al.*[11] have fitted a quadratic:

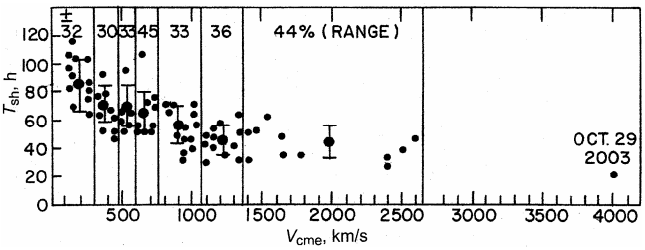

Fig. 2—Plot of transit time T_{sh} (Sun to Earth) *vs* CME (Coronal Mass Ejection) lateral expansion speed V_{cme} [The small dots are for individual events and the big dots with standard deviations are for ranges (average of 15 pairs)]

$$T_{sh} = 3.9 - 2\ V_{cme} + 2.3 \times 10^{-5}\ V^2_{cme}$$

while Schween *et al.*[13] mention a best fit as:
$T_{sh} = 203 - 20.77 \times \ln(V_{cme})$

However, the scatter around these regression lines is very large. Around the big dots in Fig. 2, the standard deviations and ranges are as given in Table 3.

Thus, whereas CMEs of low velocities (200-700 km/s) may take 60-90 h to reach the Earth's orbit, the estimates of the transit times could be wrong by ~ 30 h. The CMEs of higher velocities (900-1800 km/s) may take 30-60 h, but the estimates of the transit times could be wrong by ~ 15 h. The CMEs of very high velocities (> 2000 km/s) may take 20-30 h but the estimates of the transit times could be wrong by ~ 10 h. For the 29 Oct. 2003 event, Schwenn *et al.*[13] reported an observed transit time of ~ 19 h, ~ 5 h earlier than predicted.

(c) The CME expansion speeds (V_{cme}) have a low correlation (– 0.47) with the maximum negative Dst magnitudes as shown in Fig. 3. The small dots are for individual events and the big dots with standard deviations are for ranges (average of 15 pairs). As can be seen, the scatter is large and erratic, and any Dst value seems to be associable with any value of V_{cme}. Notably, three major Dst storms of comparable Dst values occurred at widely different values of V_{cme} (31 Mar. 2001, Dst = – 437 nT, V_{cme} ~ 942 km/s; 20 Nov. 2003, Dst = – 430 nT, V_{cme} ~ 2657 km/s; 29 Oct. 2003, Dst = – 380 nT, V_{cme} ~ 4000 km/s). Thus, the values of V_{cme} do not seem to have any consistent relationship with the Dst magnitudes. Some of the severe storms (Dst = – 150 to – 230 nT, marked with triangles) were associated with V_{cme} less than 800 km/s, while many severe storms occurred when V_{cme} was high. Thus, the geo-effectiveness of fast CMEs is somewhat higher than that of slow CMEs, but occurrences of severe storms at low or moderate V_{cme} and weak storms even at high V_{cme} are not ruled out. Using only a few events, Srivastava and Venkatakrishnan[16] reported a good correlation between CME speeds and Dst magnitudes. However, Kim *et al.*[17] used a much larger data set and found no good correlation between CME speeds and Dst magnitudes (see also Gonzalez *et al.*[18], Kane[19,20]).

Table 3—Averages of transit time T_{sh} for ascending values of V_{cme}

V_{cme}, km/s	T_{sh}, h		
	Average	Standard deviation	Range
209	87	±17 (20%)	±28 (32%)
399	71	±12 (17%)	±21 (30%)
527	69	±12 (17%)	±23 (33%)
663	67	±15 (22%)	±30 (45%)
926	57	±13 (22%)	±19 (33%)
1186	47	±10.(21%)	±17 (36%)
1864	43	±11 (26%)	±19 (44%)
4000	20	Single event	Single event

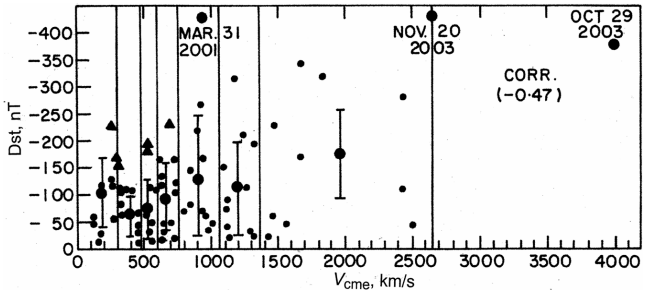

Fig. 3—Plot of the magnitudes of storm time Dst *vs* CME (Coronal Mass Ejection) lateral expansion speed V_{cme} [The small dots are for individual events and the big dots with standard deviations are for ranges (average of 15 pairs). Triangles represent moderate Dst storms associated with low V_{cme}.]

(d) For geomagnetic storms, the relevant velocities (if at all) would be V_{sh} of the IP shocks near Earth rather than of the CMEs near the Sun. However, the correlation between V_{sh} and Dst is also low (– 0.50), comparable to that of V_{cme} (– 0.47). A plot of Dst magnitudes versus V_{sh} (not shown here) showed a scatter just like the scatter in Fig. 3. It is concluded, therefore, that velocities are not of great relevance for Dst magnitudes. For the Halloween events and the 31 Mar. 2001 event having similar Dst values,

the V_{sh} values and Dst values were: (31 Mar. 2001, Dst = – 437 nT, V_{sh} = 617 km/s; 20 Nov. 2003, Dst = – 430 nT, V_{sh} = 700 km/s; 29 Oct. 2003, Dst = – 380 nT, V_{sh} ~ 2000 km/s) (see more detailed discussion in Kane[20]).

(e) The CME expansion speeds (V_{cme}) as well as the transit time of the CME up to the IP shock have very low correlations (< 0.20) with the time intervals from IP shock to maximum negative Bz (Shock-Bz) or from IP shock to maximum negative Dst (Shock-Dst). Thus, it seems to be irrelevant how much time the CME took to reach the Earth's orbit; the further evolution of a magnetic storm seems to follow its own course.

(f) The best correlation (+ 0.85) seems to be between the maximum negative magnitudes of Bz and Dst as shown in Fig. 4. The small dots are for individual events and the big dots with standard deviations are for ranges (average of 18 pairs). For low Bz values, there is considerable scatter, which could be because of the inaccuracies of the Bz values. For higher Bz values, the scatter is smaller. A linear regression fit is as follows:

$$Dst = (2.5 \pm 9.0) + (6.5 \pm 0.4)\ Bz$$

This result is not new. Relations between maximum negative Bz and Dst have been copiously studied and reported earlier by many workers (for example, Kane[20]; Cane *et al.*[21]; Wu *et al.*[22]; Su Yeon and Yu[23]; Gonzalez and Echer[24]; Howard and Tappin[25], etc.). The conclusions are for a range from moderate to very good correlations, probably because different samples are used, and the scatter in Fig. 4 is substantial.

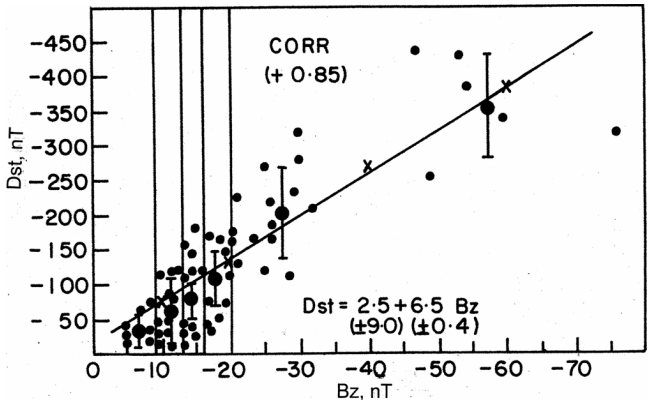

Fig. 4—Plot of negative magnitudes of Dst *vs* negative magnitudes of Bz [The small dots are for individual events and the big dots with standard deviations are for ranges (average of 18 pairs)]

Instead of Bz, the factor V_{sh}Bz was used, but the correlation was about the same (+ 0.73) which again indicates that velocities are not of much importance and negative Bz alone dominates Dst values. Gopalswamy[26] reported the best correlation using $V_{sh} \times$ Bz and Dst.

4 Phase shift of maximum negative Bz and Dst with respect to IP shock timing

Whereas the transit time of the CME from Sun to Earth (IP shock) is highly variable, it has no relationship with the further time intervals from IP shock to the following maximum negative Bz and further to maximum negative Dst (very low correlations, as seen in Table 1). Nevertheless, it may be useful to know how much time interval is involved between the IP shock arrival and maximum negative Bz (Shock to Bz), maximum negative Dst (Shock to Dst) and between maximum negative Bz and negative Dst (Bz to Dst). It was noticed that these intervals varied in a large time range. Figure 5 shows the histograms (occurrence frequency in different time ranges) for Shock to Bz, Bz to Dst, and Shock to Dst, separately for different levels of Dst, the bottom plot being for very severe storms (Dst < – 200 nT, 13 events). The following may be noted in Fig. 5:

(i) The intervals from IP shock arrival to maximum negative Bz (first column) and maximum negative Dst (third column) vary in a very wide range (0-45 h).

(ii) The average values decrease with increasing strength of Dst. In the first column, the average interval Shock to negative Bz, decreased from 10.1 h for very weak storms (0 to –50 nT, top plot) to 5.5 h for very severe storms (> 200 nT, bottom plot). In the third column, the average interval Shock to negative Dst, decreased from 14.9 h for very weak storms (0 to –50 nT, top plot) to 10.1 h for very severe storms (> 200 nT, bottom plot).

(iii) In the second column, the average interval negative Bz to negative Dst, was almost constant near about 5 h from very weak storms (0 to – 50 nT, top plot) to very severe storms (> 200 nT, bottom plot). Thus, Dst storms follow negative Bz mostly within 0-5 h.

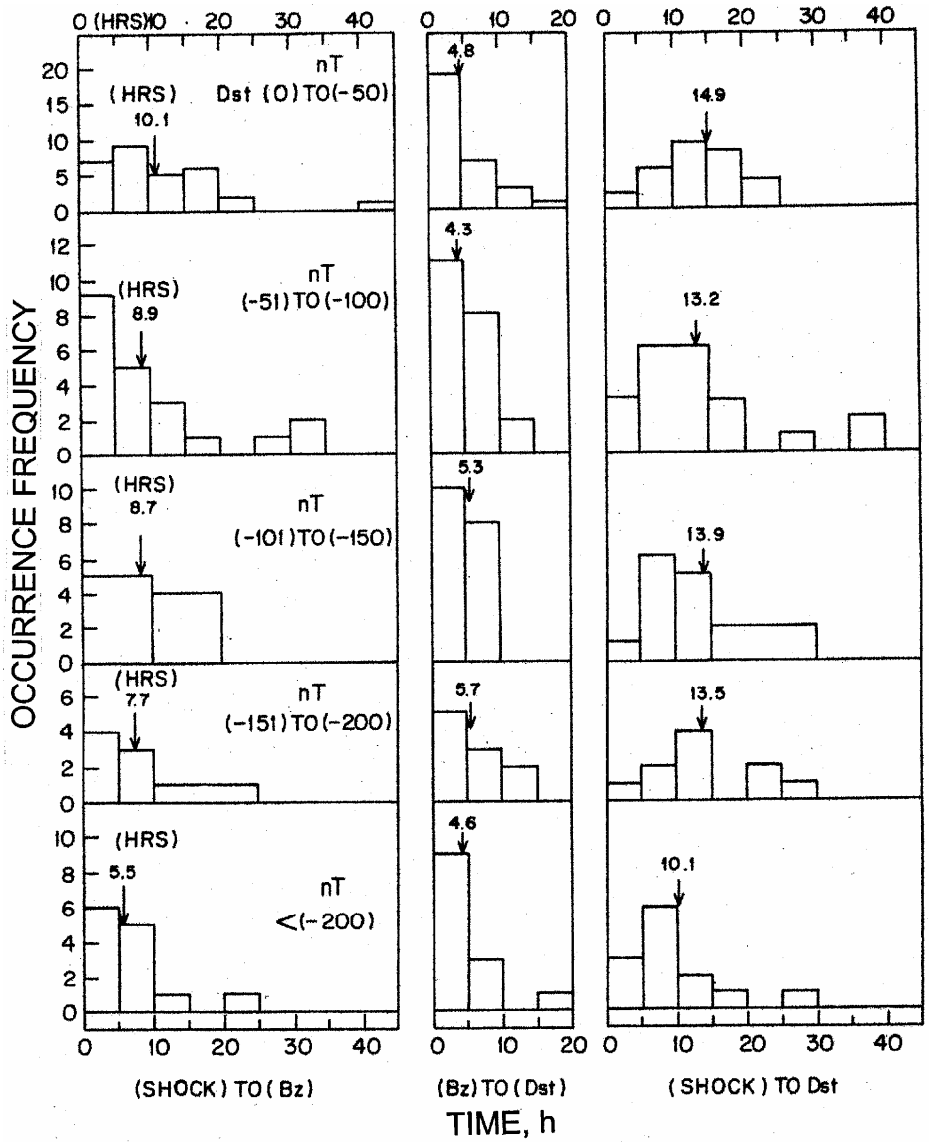

Fig. 5—Histograms (occurrence frequency in different time ranges) for Shock to Bz (first column), Bz to Dst (second column), and Shock to Dst (third column), separately for different levels of Dst (0 to – 50 nT, – 51 to – 100 nT, – 101 to – 150 nT, – 151 to – 200 nT and < 200 nT), the bottom plot being for very severe storms (Dst < – 200 nT, 13 events)

5 Other time-markers

There are some other time-markers which could give warning about impending storms, as follows:

5.1 SSC events

Since many decades, the occurrence of SSC (storm sudden commencement) has been the most spectacular part of a magnetogram. It is in the form of a sudden increase in geomagnetic field of a few tens of nT within a few minutes, heralding stormy conditions. However, there are some drawbacks:

(i) The SSC occurs when the Earth enters an IP shock. In quiet times, the sunward magnetopause extends to about 10 Earth radii. With the arrival of an IP shock, geomagnetic field is compressed further and in extreme cases, the sunward magnetopause may come down to 6-7 Earth radii. However, further development of a storm depends upon the occurrence of a negative Bz component. If this occurs, the SSC has an antecedence of a few tens of minutes before the main phase of the storm; but if Bz negative does not occur, the Dst main phase will not occur and the SSC would prove to be a false signal.

(ii) The SSC indicates entrance of the Earth in an IP shock. Before the satellite era, this was an important indicator, but with satellites like the ACE which are

nearer to the Sun, the storm warning comes about half an hour earlier than the actual arrival of the IP shock at the Earth´s orbit. Thus, SSC as an indicator of an impending storm has lost its antecedence value, compared to what it was before the satellite age.

5.2 SEP events

Solar flares sometimes cause acceleration of particles and these SEPs (solar energetic particles) follow the Archimedes spirals of interplanetary magnetic fields and reach Earth rapidly, much before the IP shock reaches the Earth´s orbit. Thus, these have an antecedence potential. There are some complications. These particles have a wide energy spectrum and particles of different energies are deflected differently in geomagnetic field and land in different proportions at the different locations, where cosmic ray neutron monitors detect the SEPs. These SEP events have been studied extensively[27,28,29] regarding their relationship with the magnitudes of associated geomagnetic storms. However, the operators of neutron monitors at different locations have to be vigilant to detect the slightest increases in their cosmic ray intensities (generally, these are substantial, several percent to several times) and issue a warning of an impending IP shock well before the actual arrival of the shock at the Earth´s orbit. Some uncertainties of a few tens of minutes will still be involved.

5.3 Cosmic ray anisotropies

Cosmic ray intensities measured by neutron monitors show Forbush decreases which look very much like Dst storms. Both have a common origin, namely entry of the Earth in an IP shock, with the major difference that Dst storm is related to the negative Bz component, while Forbush decrease is related to the total magnetic field B inside the IP shock. Recently, cosmic ray measurements with directional muon telescopes (details in Kane[30]) have shown that if an IP shock exists between the Sun and the Earth, the cosmic rays passing through the shock region show a modulation (reduction) detected by the muon telescope pointed in that direction. Thus, an impending storm can be anticipated with considerable antecedence.

6 Conclusions and discussion

Several decades back, Chapman and Bartels[5] observed that after the eruption of a solar flare, solar corpuscular radiation (particles) may affect the geomagnetic field after a few tens of hours. When CMEs (coronal mass ejections) were discovered, a measurement of the lateral expansion speeds of halo CMEs seemed to be related to the transit time of the CME from the Sun to the Earth. In the present paper, results of the examination of data for about 100 events in solar cycle 23 (1996 onwards) when CMEs and IP (Interplanetary) shocks could be matched (Manoharan *et al.*[11]; Manoharan[12]) are presented. The following were noticed:

(i) The CMEs had a large range of speeds (200-4000 km/s), but the slow CMEs seemed to be accelerated and the fast ones decelerated during the transit from Sun to Earth. Hence, IP shock speeds were in a narrower range (~ 450-2000 km/s).

(ii) A regression equation can be established between the CME lateral expansion speed and the corresponding IP shock speed; but observed values have a considerable scatter, and can have extreme deviations of ~ 35% from the predicted values.

(iii) The transit times from Sun to Earth also have a relationship with CME lateral expansion speeds; but here too, the observed values can have extreme deviations of ~ 35% from the predicted values. However, in terms of hours, the deviations from prediction are much less than the vague estimates from solar flare observations alone (few tens of hours).

(iv) Brueckner *et al.*[31], based on eight cases then known, concluded that the travel time of most CMEs from the Sun to the Earth (measured from the first appearance in C2 images to the beginning of the maximum Kp index of an associated geomagnetic storm) always amounts to about 80 h, regardless of the halos' behaviour close to the Sun. This is not true. The transit times can be as low as 25 h (extreme uncertainty ~ 5 h) to as high as 100 h (extreme uncertainty ~ 35 h).

(v) The transit times has no certain relationship with the magnitudes of the Dst storms that follow, or with the time intervals between the IP shock arrival and the following maxima of negative Bz or negative Dst. Very severe storms seem to be generally associated with fast CMEs, but some moderate storms are associated with slow CMEs and some fast CMEs are associated with weak storms.

(vi) The time intervals between IP shock arrival and the following maxima of negative Bz and Dst seem to be smaller for more severe Dst storms.

(vii) The time intervals between maximum negative Bz and maximum negative Dst are mostly in the range of 0-5 h.

(viii) The magnitudes of the maxima of negative Bz and the following negative Dst are highly correlated, indicating this as a major, overpowering relationship for determining the severeness of geomagnetic storms.

The CMEs at the Sun have a variety of characteristics and these get considerably modified during the transit up to the Earth's orbit, so that the ICMEs (Interplanetary CMEs) have IP shocks with characteristics of their own, different from those of CMEs. Further, for geo-effectiveness, the most effective parameter is the negative Bz component of interplanetary field. This feature is important only because of the peculiar geometry with respect to terrestrial magnetic field. In the geomagnetic tail, interplanetary negative Bz can neutralize geomagnetic field in the equatorial plane, thus allowing solar wind particles to enter the magnetosphere. However, for the interplanetary shock, Bz negative has no particular significance and it may assume substantial values of and on, in a random way (or perhaps systematically at fixed intervals, when magnetic field rotates in a magnetic cloud, a special subset of interplanetary abnormal structures). Thus, the evolution of Bz is unpredictable, except that in a general way, an interplanetary structure with large total magnetic field B is likely to have a substantial negative Bz some time or other, though not continuously. Fast CMEs may produce stronger IP shocks with strong interplanetary field B and perhaps a strong negative Bz; but there have been some glaring exceptions. The event of 4 Aug. 1972, was one of the fastest (transit time 14.6 h, IP shock speed ~ 2000 km/s) but the Bz component fluctuated a lot from north to south and back (Tsurutani *et al.*[32]) and resulted in a paltry Dst of – 125 nT.

Among the terrestrial damages from severe storms, the most serious one is the burnout of transformers. One way to avoid it is to switch off the transformers during the peak of a severe storm. Some embarrassing, delicate situations arise. As soon as a halo CME is noticed, its lateral expansion speed can be measured and an estimate of the transit time obtained. One may switch off the transformer just before the elapse of this time, but the IP shock may appear a few hours earlier and the transformer may get burnt prematurely. If one allows for a few hours antecedent error, the transformer may be switched off that much earlier, but every hour of power loss implies a loss of billions of dollars. So, where does one draw the line? May be the electric companies involved use their own discretion and find compromise solutions (Beland[33]; Boetler *et al*.[34]).

Acknowledgements

Thanks are due to the World Data Center for Geomagnetism, Kyoto for the Dst (SYM) Index and to the ACE SWEPAM and MAG instrument teams and the ACE Science Center for the ACE solar wind data. This work was partially supported by Fundação Nacional de Desenvolvimento Científico e Tecnológico (FNDCT), Brazil, under contract FINEP-537/CT.

References

1 Dungey J W, Interplanetary magnetic field and the auroral zones, *Phys Rev Lett (USA)*, 6 (1961) 47.

2 Carrington R C, Description of a singular appearance seen in the Sun on September 1, 1859, *Mon Not R Astron Soc (UK)*, 20 (1859) 13.

3 Hodgson R, On a curious appearance seen on the Sun, *Mon Not R Astron Soc (UK)*, 20 (1859) 15.

4 Hale G E, The spectrohelioscope and its works, part III, Solar eruptions and their apparent terrestrial effects, *Astrophys J (USA)*, 73 (1931) 379.

5 Chapman S & Bartels J, *Geomagnetism*, vol. 1 (Oxford University Press, New York), 1940, 328.

6 Parker E N, Extension of the solar corona into interplanetary space, *J Geophys Res (USA)*, 64 (1959) 1675.

7 Tousey R, *The Solar Corona*, Eds. M J Rycroft & S K Runcom (Springer-Verlag, New York), 1973, p 173.

8 Gopalswamy N, Lara A, Yashiro S & Howard R A, Coronal mass ejections and solar polarity reversal, *Astrophys J (USA)*, 598 (2003a) L63.

9 Gopalswamy N, Lara A, Yashiro S, Nunes, S & Howard R A, *Coronal mass ejection activity during Solar Cycle 23* in Proceedings of the ISCS 2003 Symposium, Solar Variability as an Input to the Earth's Environment, Tatranskà Lomnica, *Slovakia*, ESA SP-535, September, 2003, Ed. Wilson (ESTEC, Noordwijk, The Netherlands) 2003b, 403.

10 Dal Lago A, Vieira L E A, Echer E, Gonzalez W D, De Gonzalez A L C, Guarnieri F L, Schuch N J & Schwenn R, Comparison between halo CME expansion speeds observed on the Sun, the related shock transit speeds to Earth and corresponding ejecta speeds at 1 AU, *Solar Phys (Holland)*, 222 (2004) 323.

11 Manoharan P K, Gopalswamy N, Yashiro S, Lara A, Michalek G & Howard R A, Influence of coronal mass ejection interaction on propagation of interplanetary shocks,

J Geophys Res (USA), 109 (2004) A06109, DOI:10.1029/ 2003JA010300.

12 Manoharan P K, Evolution of coronal mass ejections in the inner heliosphere: A study using white light and scintillation images, *Solar Phys (Holland)*, 235 (2006) 345.

13 Schwenn R, Dal Lago A, Huttunen E & Gonzalez W D, The association of coronal mass ejections with their effects near the Earth, *Ann Geophys (France)*, 23 (2005) 1033.

14 Gopalswamy N, Lara A, Lepping R P, Kaiser M L, Berdichevsky D & St.Cyr O C, Interplanetary acceleration of coronal mass ejections, *Geophys Res Lett (USA)*, 27 (2000) 145.

15 Gopalswamy N, Yashiro S, Kaiser M L, Howard R A & Bougeret J L, Radio signatures of coronal mass ejection interaction: Coronal mass ejection cannibalism? *Astrophys J (USA)*, 548 (2001) L91.

16 Srivastava N & Venkatakrishnan P, Relationship between CME speed and geomagnetic storm intensity, *Geophys Res Lett (USA)*, 29 (2002) 1287, DOI:10.1029/ 2001GL013597.

17 Kim R S, Cho K S, Moon Y J, Kim Y H, Yi Y, Dryer M, Bong S C & Park Y D, Forecast evaluation of the coronal mass ejection (CME) geoeffectiveness using halo CMEs from 1997 to 2003, *J Geophys Res (USA)*, 110 (2005) A11104, DOI:10.1029/2005JA011218.

18 Gonzalez W D, Dal Lago A, Clua de Gonzalez A L, Vieira L E A & Tsurutani B T, Prediction of peak-Dst from halo CME/magnetic cloud-speed observations, *J Atmos Sol-Terr Phys (UK)*, 66 (2004) 161.

19 Kane R P, 1977, A comparative study of geomagnetic, interplanetary and cosmic ray storms, *J Geophys Res (USA)*, 82 (1977) 561.

20 Kane R P, How good is the relationship of solar and interplanetary plasma parameters with geomagnetic storms?, *J Geophys Res (USA)*, 110 (2005) A02213, DOI:10.1029/2004JA010799.

21 Cane H V, Richardson I G & St. Cyr O C, Coronal mass ejections, interplanetary ejecta and geomagnetic storms, *Geophys Res Lett (USA)*, 27 (2000) 3591.

22 Wu C C & Lepping R P, The effect of solar wind velocity on magnetic, cloud-associated magnetic storm intensity, *J Geophys Res (USA)*, 107 (2002) 1346, DOI:10.1029/2002JA009396.

23 Su Yeon O & Yi Y, Relationships of the solar wind parameters with the magnetic storm magnitude and their association with the interplanetary shock, *J Korean Astron Soc (Korea)*, 37 (2004) 151.

24 Gonzalez W D & Echer E, A study on the peak Dst and peak negative Bz relationship during intense geomagnetic storms, *Geophys Res Lett (USA)*, 32 (2005) L18103, DOI:10.1029/2005GL023486.

25 Howard T A & Tappin S J, Statistical survey of earthbound interplanetary shocks, associated coronal mass ejections and their space weather consequences, *Astron Astrophys (USA)*, 440 (2005) 373.

26 Gopalswamy N, Coronal mass ejections of solar cycle 23, *J Astrophys Astron (USA)*, 27 (2006) 243.

27 Smith Z, Murtagh W & Smithtro C, Relationship between solar wind low-energy energetic ion enhancements and large geomagnetic storms, *J Geophys Res (USA)*, 109 (2004) A01110, DOI:10.1029/2003JA010044.

28 Gleisner H & Warermann J, Solar energetic particle flux enhancements as an indicator of halo coronal mass ejection geoeffectiveness, *Space Weather (USA)*, 4 (2006) S06006, DOI:10.1029/2006SW000220.

29 Rawat R, Alex S & Lakhina G S, Low-latitude geomagnetic signatures during major solar energetic particle events of solar cycle-23, *Ann Geophys (France)*, 24 (2006) 3569.

30 Kane R P, Cosmic ray anisotropies during the Oct. 28-31, 2003 Halloween event, *Indian J Radio Space Phys*, 37 (2008) 28.

31 Brueckner G E, Howard R.A, Koomen M J, Korendyke C M, Michels D J, Moses J D, Socker D G, Dere K P, Lamy P L, Llebaria A, Bout M V, Schwenn R, Simnett G M, Bedford D K & Eyles C J, The large angle and spectroscopic coronagraph (LASCO), *Solar Phys (Holland)*, 162 (1995) 357.

32 Tsurutani B T, Gonzalez W D, Lakhina G S & Alex S, The extreme magnetic storm of 1–2 September 1859, *J Geophys Res (USA)*, 108 (2003) 1268 DOI:10.1029/ 2002JA009504.

33 Beland J, *Hydro-Quebec and geomagnetic storms: Measurement techniques, effects on transmission network and preventive actions since 1989*, paper presented to the 35th Scientific Assembly, COSPAR, Paris, July 19-25, 2004.

34 Boteler D H & Tapping K F, *Tracing space weather disturbances from the Sun through their effects on the ground*, paper presented to the 35th Scientific Assembly, COSPAR, Paris, July 19-25, 2004.